

A PHYSICAL LINK BETWEEN JET FORMATION AND HOT PLASMA IN ACTIVE GALACTIC NUCLEI

QINGWEN WU¹, XINWU CAO², LUIS C. HO³ AND DING-XIONG WANG¹
Accepted by ApJ, printed on August 13, 2018

ABSTRACT

Recent observations suggest that in black hole X-ray binaries jet/outflow formation is related to the hot plasma in the vicinity of the black hole, either in the form of an advection-dominated accretion flow at low accretion rates or in a disk corona at high accretion rates. We test the viability of this scenario for supermassive black holes using two samples of active galactic nuclei distinguished by the presence (radio-strong) and absence (radio-weak) of well-collimated, relativistic jets. Each is centered on a narrow range of black hole mass but spans a very broad range of Eddington ratios, effectively simulating, in a statistical manner, the behavior of a single black hole evolving across a wide spread in accretion states. Unlike the relationship between the radio and optical luminosity, which shows an abruptly break between high- and low-luminosity sources at an Eddington ratio of $\sim 1\%$, the radio emission—a measure of the jet power—varies continuously with the hard X-ray (2–10 keV) luminosity, roughly as $L_R \propto L_X^{0.6-0.75}$. This relation, which holds for both radio-weak and radio-strong active galaxies, is similar to the one seen in X-ray binaries. Jet/outflow formation appears to be closely linked to the conditions that give rise to the hot, optically thin coronal emission associated with accretion flows, both in the regime of low and high accretion rates.

Subject headings: accretion, accretion disks—black hole physics—galaxies: active—galaxies: jets—X-rays: binaries

1. INTRODUCTION

The ratio of radio to optical flux in active galactic nuclei (AGNs) spans a very wide distribution, and is possibly bimodal; radio-loud (RL) AGNs are about $10^3 - 10^4$ times brighter in the radio than radio-quiet (RQ) AGNs with the same optical emission (e.g., Kellermann et al. 1994; Xu et al. 1999). The physical origin of the RL/RQ dichotomy is still an unresolved problem in AGN physics. One possible explanation is that RL AGNs are driven by fast-rotating black holes (BHs) through the Blandford-Znajek mechanism (Blandford & Znajek 1977), while BHs in RQ AGNs are non-spinning or spinning slowly. A radio-loudness parameter of $R \equiv F_{5 \text{ GHz}}/F_B \simeq 10$ is usually taken as the division between bright RL and RQ quasars, where $F_{5 \text{ GHz}}$ is the monochromatic flux density at 5 GHz and F_B is the optical B -band flux density at 4400 Å (Kellermann et al. 1994). Extending the above R parameterization to low-luminosity AGNs (LLAGNs), however, is not straightforward, as most LLAGNs qualify as RL according to the above R criterion when their nuclear emission at radio and optical wavelengths are considered (Ho & Peng 2001; Ho 2002), even though the majority of LLAGNs generally have very low radio powers and do not have well-collimated, large-scale jets (Ho 2008). Thus, the traditional definition of radio-loudness ($R = 10$) cannot distinguish LLAGNs from classical RL AGNs such as Fanaroff & Riley (1974, FR) type I and II sources. Sikora et al. (2007) proposed that the critical value of R that divides RL and RQ sources may depend on Eddington ratio, $L_{\text{bol}}/L_{\text{Edd}}$, where L_{bol} is the bolometric luminosity and the Eddington luminosity

$L_{\text{Edd}} = 1.28 \times 10^{38} (M_{\text{BH}}/M_{\odot}) \text{ erg s}^{-1}$. To avoid possible confusion regarding the definition of RL versus RQ, in this work we simply use the terms “radio-strong” (RS) and “radio-weak” (RW) to distinguish between sources that have highly relativistic, well-collimated jets (e.g., blazars, FR I and FR II radio galaxies, and classical RL quasars) and from those that do not (e.g., Seyfert galaxies and classical RQ quasars), regardless of Eddington ratios or luminosities.

AGNs are powered by accretion of matter onto BHs, as are X-ray binaries (XRBs). Both the optical/UV bumps observed in quasars and the soft X-ray emission observed in the high/soft (HS) state of XRBs can be naturally interpreted as multi-temperature blackbody emission from a cold, optically thick, geometrically thin standard accretion disk (SSD, Shakura & Sunyaev 1973). Models of hot, optically thin, geometrically thick advection-dominated accretion flows (ADAFs; also called radiatively inefficient accretion flows) have been developed for BHs accreting at low mass accretion rates (e.g., Ichimaru 1977; Narayan & Yi 1994, 1995; Abramowicz et al. 1995; see Kato et al. 2008 and Narayan & McClintock 2008 for recent reviews). The ADAF model can successfully explain most observational features of nearby LLAGNs and XRBs in their LH state (e.g., Quataert et al. 1999; Yuan et al. 2005; Wu et al. 2007; Ho 2009; Yu et al. 2011; Xu 2011; Nemmen et al. 2012; Liu & Wu 2013; see reviews in Remillard & McClintock 2006, Done et al. 2007, Yuan 2007, Ho 2008). For Eddington ratios lower than a critical value of $\sim 1\%$, the hard X-ray (2–10 keV) photon indices of both XRBs and AGNs are inversely correlated with the Eddington ratio; the trend reverses for sources with

¹ School of Physics, Huazhong University of Science and Technology, Wuhan 430074, China; Email: qwwu@hust.edu.cn; dxwang@hust.edu.cn

² Key Laboratory for Research in Galaxies and Cosmology, Shanghai Astronomical Observatory, Chinese Academy of Sciences, 80 Nandan Road, Shanghai, 200030, China; cxw@shao.ac.cn

³ The Observatories of the Carnegie Institution for Science, 813 Santa Barbara Street, Pasadena, CA 91101, USA; lho@obs.carnegiescience.edu

Eddington ratios $\gtrsim 1\%$ (e.g., Wu & Gu 2008; Gu & Cao 2009; Sobolewska & Papadakis 2009; Younes et al. 2011, and references therein). The different correlations between X-ray spectral slope and Eddington ratio found in high-luminosity and low-luminosity sources are roughly consistent with the expectations from the SSD/corona model (Cao 2009) and the ADAF model (Qiao & Liu 2013), respectively. They provide strong evidence for accretion mode transitions in BH accreting systems. Accretion mode transitions also offer a plausible explanation for the trends between jet power and BH mass observed in different classes of powerful RL AGNs (e.g., Ghisellini & Celotti 2001; Wu & Cao 2008; Xu et al. 2009).

Simultaneous multi-wavelength observations of BH XRBs in their LH state have shown that their radio luminosity is correlated with their X-ray luminosity, roughly as $L_R \propto L_X^{0.6}$ (Corbel et al. 2003; Gallo et al. 2003). Once the sources enter the HS state, their radio emission becomes quenched, such that L_R is significantly depressed at a given L_X (e.g., Fender et al. 1999; Corbel et al. 2000). The observed radio properties of XRBs suggest that, apart from the possible influence of BH spin, jet formation is somehow also regulated by accretion rate. In an important recent study, Zdziarski et al. (2011) found that the radio–X-ray correlation in the BH XRB Cygnus X-1 extends to the HS state only if its hard X-ray emission is considered (after subtracting the blackbody component due to the SSD). Their result suggests that the radio emission is related only to the hot plasma in accretion flows (e.g., ADAF or corona above the SSD). In such a scenario, the suppression of radio emission during in the HS state in XRBs may be caused by a reduction of the corona resulting from its being cooled by the high luminosity of the SSD in the HS state. A similar phenomenon is seen in AGNs: the ratio coronal emission (represented by the hard X-rays) to the bolometric luminosity decreases with increasing Eddington ratio (e.g., Wang et al. 2004b; Cao 2009). Thus, the hot plasma—either in the form of an ADAF or a corona—may play a key role in regulating the radio emission in both XRBs and AGNs.

Zdziarski et al. (2011) proposed that the hot plasma (ADAF/corona), not the cold SSD, controls the formation of a jet or outflow. One practical difficulty in testing this hypothesis further is that radio emission is too weak to be detected in most XRBs in their HS state. By contrast, radio data are much more readily available for supermassive BHs, across a wide range of accretion rates. Indeed, the existence of the so-called BH fundamental plane relation linking radio and X-ray emission to BH mass suggests that the physics of accretion and jet formation can be unified across a very wide mass range, stretching from XRBs to AGNs (Merloni et al. 2003; Falcke et al. 2004). In light of this, it should be possible to use AGNs to test Zdziarski’s hot plasma scenario for jet/outflow formation. However, it should be noted that differences in BH mass or accretion rate alone still cannot fully explain the radio dichotomy in AGNs; other parameters, such as BH spin or the strength of the large-scale magnetic field, may also play a key role (e.g., Spruit 2010; Broderick & Fender 2011).

We carefully assemble an AGN sample to test the viability of the hot plasma jet/outflow formation. A Λ CDM cosmology with $H_0 = 70 \text{ km s}^{-1} \text{ Mpc}^{-1}$, $\Omega_m = 0.27$, and

$\Omega_\Lambda = 0.73$ is adopted in this work.

2. SAMPLE

To allow for the possibility of a radio dichotomy, we explore the relation between jets and accretion processes separately for RS and RW sources. We impose two selection criteria for each sample: (1) that the sources span a narrow range of BH masses (± 0.4 dex) and (2) that they cover as wide a range of luminosities as possible to mimic a large dynamic range in accretion rate or Eddington ratio at a fixed mass. The spread of 0.4 dex in BH mass was chosen to reflect the typical uncertainty in current methods of estimating M_{BH} , either from broad emission lines for type 1 AGNs (e.g., Vestergaard & Peterson 2006) or from the $M_{\text{BH}} - \sigma_*$ (e.g., Gültekin et al. 2009; Ho 2009) or $M_{\text{BH}} - L_{\text{bulge}}$ (e.g., Marconi & Hunt 2003) relation for type 2 AGNs and very low-luminosity AGNs. We note that our samples are selected from the literature and are quite heterogeneous and incomplete. Nevertheless, the main conclusions of this work do not depend on the statistical completeness of the sample. We describe the RW and RS samples separately below.

2.1. RW AGNs

The RW sample, summarized in Table 1, includes both bright, low-redshift type 1 AGNs (classical Seyfert 1s and quasars) and nearby LLAGNs (low-luminosity Seyferts and LINERs) without evident large-scale, well-collimated jets. We construct a sample of 52 RW AGNs with BH masses lying in the narrow range $M_{\text{BH}} = 10^{8 \pm 0.4} M_\odot$, using the AGN catalogs from CAIXA (Bianchi et al. 2009) and the Palomar spectroscopic survey of nearby galaxies (Ho et al. 1995). These samples have well-determined multiwavelength observations and BH mass estimates. The average BH mass, $10^8 M_\odot$, is chosen to optimize both the size and the luminosity coverage of the sample.

We select 25 optically bright type 1 AGNs from the CAIXA catalog, for which BH masses, radio core flux densities, and absolute V magnitudes are available (Bianchi et al. 2009, and references therein). The BH masses of these type 1 AGNs are calculated from the virial product of the velocity widths of the broad $H\beta$ emission line and the size of the broad-line region estimated from the size-luminosity relation of reverberation-mapped AGNs (Kaspi et al. 2000, 2005); typical uncertainties in the mass estimates are ~ 0.4 dex (e.g., Vestergaard & Peterson 2006; McGill et al. 2008). We obtain B -band luminosities from the V absolute magnitudes and $B - V$ colors given in Bianchi et al. (2009); we assume $B - V = 0.3$ mag if no color information is available. We additionally make use of 2–10 keV X-ray luminosities from Zhou & Zhang (2010), which are derived from targeted observations from *XMM-Newton*.

We add an additional 27 LLAGNs from the literature to increase the luminosity coverage of the sample. Most of the sources are taken from the Palomar survey (Ho et al. 1995), which has well-determined multiwavelength data, including interferometric radio observations (e.g., Ho & Ulvestad 2001; Ho 2002; Nagar et al. 2005) and X-ray observations from *Chandra* or *XMM-Newton* (e.g., Ho et al. 2001; Panessa et al. 2006; Ho 2009). As emphasized in Ho (2008), high-resolution data are essen-

Table 1. Data for RW AGNs

Name	z or D_L^a (Mpc)	$\log L_{2-10\text{keV}}$ (ergs^{-1})	$\log L_{5\text{ GHz}}$ (ergs^{-1})	$\log L_B$ (ergs^{-1})	$\log R$	$\log M_{\text{BH}}$ (M_{\odot})	Refs. ^b
Ark 120	0.0323	43.95	38.56	44.17	-5.61	8.27	1,2,2,2
Ark 374	0.0630	43.49	38.67	44.26	-5.59	7.86	1,2,2,2
Fairall 9	0.0470	43.97	39.11	44.52	-5.41	7.91	1,2,2,2
H0557-385	0.0339	44.03	39.42	43.51	-4.09	7.64	1,2,2,2
MC-5-23-16	0.0085	43.02	37.68	42.83	-5.15	7.85	1,2,2,2
Mrk 79	0.0222	43.12	38.35	43.67	-5.32	8.01	1,2,2,2
Mrk 279	0.0305	43.50	38.93	43.78	-4.85	7.62	1,2,2,2
Mrk 290	0.0296	43.25	38.34	43.85	-5.51	7.65	1,2,2,2
Mrk 509	0.0344	44.68	38.83	44.61	-5.78	7.86	1,2,2,2
Mrk 841	0.0364	43.89	38.18	44.20	-6.02	7.88	1,2,2,2
Mrk 1014	0.1630	43.85	40.45	44.86	-4.41	8.03	1,2,2,2
NGC 2992	0.0077	42.97	38.83	43.67	-4.84	7.72	1,2,2,2
NGC 5548	0.0172	43.39	38.70	43.60	-4.90	8.03	1,2,2,2
NGC 7213	0.0060	42.27	38.96	43.18	-4.22	7.99	1,2,2,2
PG 0052+251	0.1550	44.61	39.50	45.01	-5.51	8.40	1,2,2,2
PG 0804+761	0.1000	44.46	39.40	44.89	-5.49	8.24	1,2,2,2
PG 0953+414	0.2341	44.73	40.17	45.57	-5.40	8.24	1,2,2,2
PG 1048+342	0.1670	44.04	37.57	44.87	-7.30	8.37	1,2,2,2
PG 1115+407	0.1550	43.93	38.98	44.73	-5.75	7.67	1,2,2,2
PG 1307+085	0.1550	44.08	39.10	45.17	-6.07	7.90	1,2,2,2
PG 1322+659	0.1680	44.02	38.88	44.97	-6.09	8.28	1,2,2,2
PG 1402+261	0.1640	44.15	39.56	45.02	-5.46	7.94	1,2,2,2
PG 1415+451	0.1140	43.60	38.82	44.18	-5.36	8.01	1,2,2,2
PG 1427+480	0.2210	44.20	38.14	44.51	-6.37	8.09	1,2,2,2
PG 1501+106	0.0364	43.69	39.00	44.20	-5.20	7.88	1,2,2,2
NGC 224 (M31)	0.7	35.85	32.10	—	—	7.82	3,4,5
NGC 266	62.4	40.87	37.78	—	—	8.37	6,7,5
NGC 821	23.2	38.30	35.40	—	—	8.21	8,8,5
NGC 1097	14.5	40.63	36.29	—	—	8.08	6,7,5
NGC 1667	61.2	40.55	37.40	40.86	-3.46	7.81	3,9,10,5
NGC 2787	13.0	38.31	36.40	38.90	-2.50	8.14	11,12,4,5
NGC 2841	12.0	38.30	36.00	39.34	-3.34	8.31	8,8,10,5
NGC 3031	1.4	39.41	36.21	39.41	-3.20	7.73	11,12,4,5
NGC 3147	40.9	41.87	38.01	40.52	-2.51	8.29	3,9,10,5
NGC 3169	19.7	41.05	37.20	39.39	-2.19	8.01	3,4,10,5,
NGC 3245	22.2	39.29	36.98	40.06	-3.08	8.21	3,4,4,5
NGC 3379	8.1	37.53	35.73	38.70	-2.97	8.18	3,4,4,5
NGC 4143	17.0	40.03	37.18	41.15	-3.97	8.16	3,7,10,5
NGC 4168	16.8	38.97	36.93	38.96	-2.03	7.97	13,9,14,5
NGC 4203	9.7	40.80	36.70	39.80	-3.10	7.79	15,12,4,5
NGC 4216	16.8	38.91	36.79	—	—	8.09	3,16,5
NGC 4235	35.1	42.25	37.57	40.87	-3.30	7.60	13,9,10,5
NGC 4459	16.8	38.87	36.09	39.30	-3.21	7.82	3,4,4,5
NGC 4477	16.8	39.60	35.64	39.58	-3.94	7.89	3,9,10,5
NGC 4501	16.8	39.59	36.25	39.62	-3.37	7.79	3,9,10,5
NGC 4579	16.8	41.51	37.81	40.72	-2.91	7.77	3,9,9,5
NGC 4621	16.8	37.80	35.10	—	—	8.34	17,8,5
NGC 4636	17.0	39.38	36.4	39.90	-3.50	8.14	3,16,10,5
NGC 4697	12.4	37.30	35.00	—	—	7.83	17,8,5
NGC 5033	18.7	41.08	38.00	41.40	-3.40	7.60	13,9,10,5
NGC 7582	22.3	41.69	38.55	—	—	7.67	18,8,5
NGC 7603	124.2	43.65	39.00	42.10	-3.10	8.14	19,4,4,5

Note. — ^a The distances of nearby LLAGNs are adopted from Ho (2009).

^b References for X-ray, radio, and optical luminosities, and BH mass, respectively: (1) Zhou & Zhang (2010); (2) Bianchi et al. (2009); (3) Ho (2009); (4) Ho (2002); (5) the BH mass is estimated from the $M_{\text{BH}} - \sigma_*$ relation of Gültekin et al. (2009), adopting σ_* values from Ho (2009) except for four sources (NGC 1097, NGC 4697, NGC 7582, and NGC 7603), which were taken from the Hyperleda database; (6) Eracleous et al. (2010); (7) Nemmen et al. (2013); (8) Yuan et al. (2009); (9) Ho & Ulvestad (2001); (10) the optical B -band luminosity is estimated from the total $H\beta$ luminosity in this work; (11) Ho et al. (2001); (12) Sikora et al. (2007); (13) Panessa et al. (2006); (14) Ho & Peng (2001); (15) Pian et al. (2010); (16) Nagar et al. (2005); (17) Wrobel et al. (2008); (18) Gültekin et al. (2009); (19) Malizia et al. (2007).

tial to properly isolate the low-level nuclear component of the LLAGN from the often much brighter emission from the surrounding host galaxy. Since high-resolution optical continuum measurements are not uniformly available for the Palomar galaxies, we estimate the optical luminosities of the LLAGNs from their $H\beta$ line luminosity, using the correlation between $L_{H\beta}$ and M_B for both bright and faint type 1 AGNs, as calibrated by Ho & Peng (2001). We

take the $H\beta$ luminosities directly from Ho (2002) when available; otherwise, we derive $H\beta$ from the extinction-corrected total $H\alpha$ luminosity (narrow plus broad component, if present) and the ratio of $H\alpha$ to $H\beta$ (Ho et al. 1997a,b, 2003). We estimate BH masses for the LLAGNs from the stellar velocity dispersion σ_* of the host galaxy bulge, using the $M_{\text{BH}} - \sigma_*$ relation of Gültekin et al. (2009), which has an intrinsic scatter of ~ 0.4 dex. Veloc-

Table 2. Data for RS AGNs (FR Is and FR IIs)

Name	z	Type	$\log L_{2-10\text{keV}}$ (ergs^{-1})	$\log L_{178\text{ MHz}}$ (ergs^{-1})	$\log M_{\text{BH}}$ (M_{\odot})	Refs.
3C 31	0.0167	I	40.67	40.31	8.70	1
3C 48	0.3670	I	45.00	43.64	9.20	1
3C 66B	0.0215	I	41.10	40.69	8.84	1
3C 83.1B	0.0255	I	41.13	40.88	9.01	1
3C 84	0.0177	I	42.91	40.92	8.64	1
3C 264	0.0208	I	41.87	40.69	8.80	1
3C 272.1	0.0029	I	39.35	38.84	8.80	1
3C 296	0.0237	I	41.49	40.51	8.80	1
3C 338	0.0303	I	42.31	41.29	8.92	1
3C 346	0.1620	I	43.40	42.15	8.89	1
3C 442A	0.0270	I	41.10	40.71	8.40	1
3C 449	0.0171	I	40.35	40.16	8.54	1
3C 465	0.0293	I	41.04	41.16	9.13	1
NGC 6251	0.0240	I	41.60	40.43	8.98	1
3C 20	0.1740	II	44.05	42.82	8.66	2
3C 33.1	0.1810	II	44.38	42.34	8.58	2
3C 47	0.4250	II	45.05	43.52	9.20	2
3C 79	0.2559	II	44.18	43.07	8.96	2
3C 171	0.2384	II	44.08	42.80	8.70	2
3C 184.1	0.1187	II	43.91	41.95	8.57	2
3C 284	0.2394	II	43.98	42.57	9.09	2
3C 285	0.0794	II	43.33	41.53	8.61	2
3C 349	0.2050	II	43.87	42.48	8.75	2
3C 436	0.2145	II	43.53	42.65	9.06	2
3C 452	0.0811	II	44.00	42.23	8.69	2
3C 457	0.4280	II	44.56	43.23	9.09	3

Note. — References for BH mass: (1) Wu et al. (2011); (2) estimated in this work; (3) McLure et al. (2004).

ity dispersions of 23 sources are available from Ho et al. (2009), and the remaining four were found in the Hyperleda database⁴ (see Table 1 for details).

2.2. RS AGNs

In order to explore the relation between relativistic jets and accretion processes in RS AGNs, it is important to isolate emission radiated separately from the jet and the disk, since the disk emission can be contaminated by the powerful jets. The nuclear emission in RS AGNs can also be Doppler boosted for relativistic jets viewed at small angles (e.g., blazars); conversely, it can be even deboosted for relativistic jets with large viewing angles (e.g., FR I/IIs). For the purpose of this work, we choose FR I and FR II radio galaxies, which are viewed at relatively large angles. In these sources the contribution of jet emission at X-ray energies should not be important due to the deboosting effect. For example, for a jet viewing angle of 45° to 90° , the jet emission can be deboosted by several tens to a thousand times for a typical jet Lorentz factor of ~ 10 (e.g., Ghisellini et al. 1993). Recent studies also suggest that the X-ray emission of FR I/IIs are dominated by accretion processes (ADAFs in FR Is and disk corona in FR IIs; Gliozzi et al. 2003; Wu et al. 2007; Hardcastle et al. 2009). To estimate the jet power, we use low-frequency radio emission because it usually originates in diffuse, optically thin radio lobes moving at low velocities, for which Doppler boosting or deboosting effects are negligible (e.g., Willott et al. 1999).

We initially select FR I/II galaxies from the 3CRR catalog, most of which have multi-waveband observations (e.g., low-frequency radio powers, host galaxy luminosity, and narrow emission-line luminosity). Hardcastle et al. (2009)

collected data for ~ 100 sources in the 3CRR catalog to investigate the nature of the nuclei of FR I/IIs that have been observed by *Chandra* or *XMM-Newton*. The X-ray spectra of these sources were fit by a two-component model if a single power law is unable to provide a satisfactory fit (for details, see Hardcastle et al. 2009). Following Hardcastle et al. (2009), we regard the heavily absorbed component as the “accretion-related” component, and we adopt the absorption-corrected X-ray luminosities in this work. We only choose FR I/IIs with well-measured absorbing column density, leaving out those with uncertain N_{H} or $N_{\text{H}} > 10^{24}\text{cm}^{-2}$ to ensure that their intrinsic X-ray emission in the 2–10 keV can be accurately measured. Barthel & Arnaud (1996) showed that low-frequency radio emission may not be a good tracer of jet power in sources with bright hot spots, as the emission of the lobes is dominated by the strong radiation of the spots. We thus exclude FR IIs with previously reported detections of hot spots in the X-ray or optical bands, as listed in Hardcastle et al. (2004, and references therein). The BH masses of the FR Is are estimated from the stellar velocity dispersion of the host and the $M_{\text{BH}} - \sigma_*$ relation. The FR IIs generally do not have measurements of σ_* available, and for these we obtain their BH masses from their *H*-band luminosity (Buttiglione et al. 2010), $M_{\text{BH}} - L_{\text{H}}$ relation of Marconi & Hunt (2003). The uncertainty of BH masses estimated from the bulge luminosity is comparable to that estimated from the $M_{\text{BH}} - \sigma_*$ relation (~ 0.4 dex; e.g., Gültekin et al. 2009).

The final RS sample consists of 26 radio galaxies (14 FR Is and 12 FR IIs) with $M_{\text{BH}} = 10^{8.8 \pm 0.4} M_{\odot}$. Again, the narrow range of mass was chosen by design, to mimic, as closely as possible, a sample with fixed M_{BH} . Table 2 lists

⁴ <http://leda.univ-lyon1.fr>

their radio luminosities at 178 MHz, hard (2–10 keV) X-ray luminosities, and BH masses. It should be noted that the RW and RS samples do not overlap in BH mass; the latter has M_{BH} higher by 0.8 dex. This is a consequence of the fact that most FR I/IIs are hosted by giant elliptical galaxies, whereas RW AGNs cover a broad range of galaxy types, both spirals and ellipticals, and hence a broader range of M_{BH} . Unfortunately, the available data do not permit us to construct a sample of RW and RS AGNs at fixed M_{BH} that simultaneously covers a wide enough luminosity range for our purposes. In what follows, we will examine the possible connection between the hot plasma and jets/outflows separately for the RW and RS samples.

3. RESULTS

The sources in the RW sample have a fixed BH mass, $M_{\text{BH}} = 10^{8.0 \pm 0.4} M_{\odot}$, and cover a wide range of Eddington ratios, $-8 \lesssim \log L_{\text{bol}}/L_{\text{Edd}} \lesssim 0$, assuming $L_{\text{bol}} = 10L_B$ (McLure & Dunlop 2004). By design, this sample is meant to mimic a single AGN experiencing a wide range of accretion rates, from very high to very low.

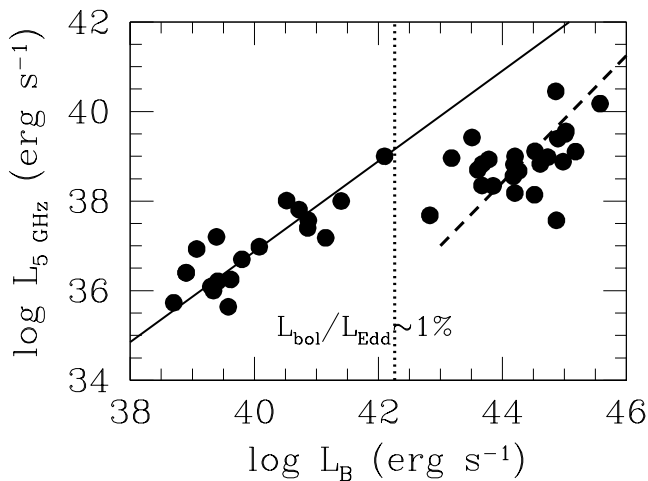


FIG. 1.— Relation between L_B and $L_{5 \text{ GHz}}$ for RW AGNs with BH masses in the range $M_{\text{BH}} = 10^{8 \pm 0.4} M_{\odot}$. The dotted line corresponds to $L_{\text{bol}}/L_{\text{Edd}} = 1\%$, assuming $L_{\text{bol}} = 10L_B$; the solid and dashed lines are the best fits for sources with $L_{\text{bol}}/L_{\text{Edd}}$ below and above this limit, respectively.

Figure 1 shows the relation between $L_{5 \text{ GHz}}$ and L_B . We find that optically luminous sources follow a different trend from weaker sources, with the two populations roughly divided at a critical Eddington ratio of $L_{\text{bol}}/L_{\text{Edd}} \approx 1\%$. The dashed and solid lines represent the best-fitting linear relation between $L_{5 \text{ GHz}}$ and L_B for sources with Eddington ratios above and below this critical limit. The regression fits assume typical uncertainties of 0.2 and 0.3 dex for the radio and optical luminosities, respectively (Ho & Peng 2001). For $L_{5 \text{ GHz}} \propto L_B^{\alpha}$, $\alpha = 1.42 \pm 0.22$ for luminous sources and $\alpha = 1.01 \pm 0.10$ for weaker sources. The two slopes are significantly different. More importantly, the luminous sources with Eddington ratios above the critical limit lie systematically offset below the best-fit line of the fainter sources below this limit. This can also be seen from examination of the distribution of the radio-loudness parameter: the R value of LLAGNs is on

average ~ 2 orders of magnitude higher than that of luminous AGNs. According to the Kolmogorov-Smirnov test, the hypothesis that the two distributions of R are drawn from the same parent population can be rejected with a probability of $p < 0.001$.

By contrast, for all but one source (M31) the 5 GHz radio luminosity is tightly correlated with the hard X-ray (2–10 keV) luminosity over 8 orders of magnitude (Figure 2). Excluding M31, the best-fit linear regression for the RW sample yields

$$\log L_{5 \text{ GHz}} = (0.58 \pm 0.02) \log L_{2-10 \text{ keV}} + (13.68 \pm 0.71), \quad (1)$$

where we assume typical uncertainties of 0.2 and 0.3 dex for the radio and X-ray luminosities, respectively (e.g., Ho & Peng 2001; Strateva et al. 2005). To ensure that the correlation between radio and X-ray luminosity is not spurious as a consequence of the mutual dependence on distance, we performed a Spearman partial correlation analysis using distance as the third variable; the probability for accepting the null hypothesis that $L_{5 \text{ GHz}}$ and $L_{2-10 \text{ keV}}$ are uncorrelated is $p = 9.8 \times 10^{-6}$. We also find that the radio and X-ray fluxes remain significantly correlated for RW AGNs, with a Spearman correlation coefficient of $\rho = 0.53$ and $p = 2.4 \times 10^{-5}$. Both of these tests suggest that the $L_{5 \text{ GHz}} - L_{2-10 \text{ keV}}$ correlation is not driven by the distance effect.

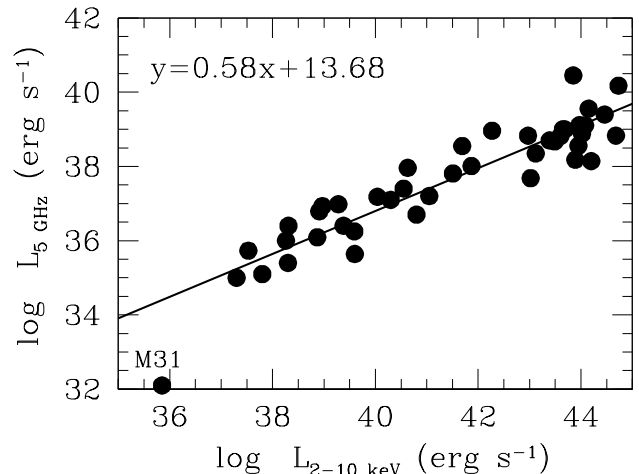


FIG. 2.— Relation between $L_{2-10 \text{ keV}}$ and $L_{5 \text{ GHz}}$ for RW AGNs with BH masses in the range $M_{\text{BH}} = 10^{8 \pm 0.4} M_{\odot}$. The solid line is the best fit for all sources, except for M31, which evidently deviates from other sources.

The RS sample, anchored at $M_{\text{BH}} = 10^{8.8 \pm 0.4} M_{\odot}$, also has a wide distribution of Eddington ratios ($-6 \lesssim \log L_{\text{bol}}/L_{\text{Edd}} \lesssim -1$). As expected, the X-ray luminosities of FR IIIs are systematically higher than those of FR Is. Figure 3 shows the relation between 178 MHz and 2–10 keV luminosities; these two quantities are tightly correlated over ~ 5 orders of magnitude in luminosity. The best fit, once again assuming uncertainties of 0.2 and 0.3 dex for the radio and X-ray luminosities, is

$$\log L_{178 \text{ MHz}} = (0.76 \pm 0.04) \log L_{2-10 \text{ keV}} + (9.94 \pm 1.85). \quad (2)$$

A Spearman partial correlation analysis confirms that this correlation is not an artifact of a mutual dependence on distance ($p = 4.3 \times 10^{-3}$), although the radio and X-ray fluxes themselves are only correlated at a mildly significant level ($\rho = 0.38$ and $p = 0.04$).

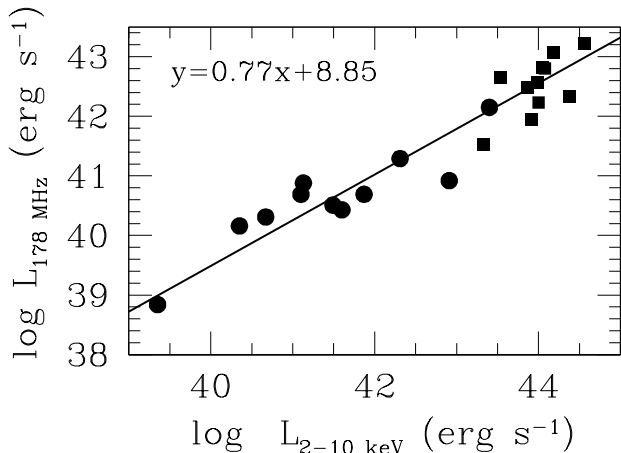


FIG. 3.— Relation between $L_{2-10 \text{ keV}}$ and $L_{178 \text{ MHz}}$ for FR I (circles) and FR II (squares) sources with BH masses in the range $M_{\text{BH}} = 10^{8.8 \pm 0.4} M_{\odot}$. The solid line is the best fit for all the sources.

4. DISCUSSION

Both highly collimated relativistic jets and less collimated nonrelativistic outflows are common features in a variety of astrophysical objects, most notably in BH XRBs and AGNs. Multi-wavelength observations of BH XRBs suggest that jet/outflow formation is closely correlated to the accretion mode in BH XRBs: jets preferentially form in the ADAF state but are suppressed when the ADAF transits to the SSD (e.g., Gallo et al. 2003; Corbel et al. 2003). In an interesting recent study, Zdziarski et al. (2011) found that the jet of the XRB Cygnus X-1 may be regulated by its hot plasma. In this work, we investigate this issue using two samples of AGNs with (RS) and without (RW) powerful relativistic jets. Each of the two samples is restricted to an essentially identical BH mass but spans a wide dynamic range in Eddington ratio. Our goal is to simulate, using a large sample of AGNs, as closely as possible the condition of a *single* supermassive BH evolving through a large variation in accretion rate. How does accretion mode transition affect the jet properties as traced through radio emission?

The optical continuum of bright RW AGNs originates mainly from the multi-temperature blackbody emission from the SSD, whereas in LLAGNs it may come from an ADAF. Thus, the relation between the radio and optical luminosity provides clues to the connection between the jet/outflow and the disk, a subject investigated by many groups (e.g., Xu et al. 1999; Ho & Peng 2001; Wang et al. 2004a; Sikora et al. 2007). In RW AGNs, the radio–optical correlation of high-luminosity sources clearly deviates from that of LLAGNs (Figure 1); they separate near a dividing line of $L_{\text{bol}}/L_{\text{Edd}} \simeq 1\%$, which roughly corresponds to the theoretical prediction for the accretion mode to transition from an ADAF at low luminosities to an SSD at high luminosities. Because the

radiative efficiency increases significantly when an ADAF switches to an SSD, the data points for the bright AGNs shift toward higher optical luminosity than the LLAGNs. Although Figure 1 gives the impression that the jet emission is strongly suppressed in bright AGNs, we suggest that two effects, in fact, contribute to this apparent offset: (1) an enhancement of the radiative efficiency as the source evolves from the LH ADAF state to the HS SSD state; (2) a genuine decrease in the efficiency of jet production at high luminosities (accretion rates). Both occur above a critical Eddington ratio threshold of $L_{\text{bol}}/L_{\text{Edd}} \simeq 1\%$, and both manifest themselves as a reduction of the radio-loudness parameter R . But instead of viewing the decline in R as caused solely by a decrease in radio power, we suggest that at least part of the relative decrease of radio to optical luminosity is actually due to the increase of the optical disk (optical/UV) emission in the HS state. Conversely, it is the reduction of the disk emission during the LH ADAF state that is partly responsible for the boost in R , an effect found in LLAGNs (Ho 1999; Ho & Peng 2001; Ho 2002). This can be seen in Figure 1 by the points that cluster around a roughly constant radio luminosity of $L_{5 \text{ GHz}} \simeq 10^{38.5 \pm 1} \text{ erg s}^{-1}$ and yet whose optical luminosities are spread over ~ 4 orders of magnitude ($L_B \approx 10^{41} - 10^{45} \text{ erg s}^{-1}$).

But this is not the whole story. As in XRBs, we believe that the radio emission in AGNs is additionally suppressed in the HS state. Similar to the case of the well-studied XRB Cygnus X-1 (Zdziarski et al. 2011), AGNs, both RW (Figure 2) and RS (Figure 3), obey a *single*, tight correlation between radio and hard X-ray luminosity across an enormous range in Eddington ratios, which formally includes systems in the LH and HS states. Parameterizing the relation as $L_R \propto L_X^\alpha$, $\alpha \approx 0.6$ for RW sources and $\alpha \approx 0.75$ for RS sources. In the case of Cygnus X-1, Zdziarski et al. (2011; see also Miller et al. 2012) proposed that the existence of a single radio–X-ray correlation that encompasses the LH and HS states implies that the jet/outflow may be controlled primarily by the hot plasma (ADAF or disk corona). The analysis presented in this paper extends this concept to supermassive BHs.

The hot plasma in the vicinity of the BH may couple naturally to the production of jets and outflows for several reasons. First, the optically thin, hot plasma in either the ADAF or the corona reaches temperatures that are nearly virial and has a positive Bernoulli parameter (e.g., Narayan & Yi 1994, 1995). Under these conditions the material can escape as an outflow (e.g., Blandford & Begelman 1999; Cao 2002; Merloni & Fabian 2002). Second, jets and outflows are driven by the large-scale poloidal magnetic field (e.g., Blandford & Znajek 1977; Blandford & Payne 1982), which, according to the dynamo theory, has a length scale comparable to the disk thickness (e.g., Meier 2001). A hot ADAF or corona, being quasi-spherical, has the geometric configuration conducive to sustaining a strong poloidal magnetic field if it is in pressure equilibrium with the thermal plasma. Finally, the radio emission may originate from the very same medium that produces the X-ray emission. For example, the radio emission may be synchrotron radiation from non-thermal electrons that are generated by turbulence, magnetic reconnection, or weak shocks in the hot plasma (e.g.,

Yuan et al. 2003; Laor & Behar 2008; Ding et al. 2010; Liu & Wu 2013). However, it is unclear whether this coronal model can explain the level of radio emission observed in powerful quasars; a forthcoming paper will address this issue.

Lastly, we note that the correlation between radio and hard X-ray emission extends to RS AGNs, which in our study are represented by FR I and FR II radio galaxies, the equivalent of ADAF-dominated and SSD-dominated sources, respectively. By analogy with the situation for the RW sources, even the highly relativistic, well-collimated jets of FR I/II radio galaxies appear to be connected to the hot plasma. We do not have novel ideas to contribute to the still unresolved physical origin for the existence of the radio dichotomy. Parameters that may be important include the large-scale magnetic field (Cao 2011) and the BH spin (e.g., Wu et al. 2011; Tchekhovskoy et al. 2011; Li

& Cao 2012; Narayan & McClintock 2012, and see Spruit 2010 for a recent review).

We thank Feng Yuan, Bifang Liu and members of HUST astrophysics group for many useful discussions and comments. This work was supported by the National Basic Research Program of China (2009CB824800), the NSFC (grants 11143001, 11103003, 11133005, 11173043, 11121062, 10833002 and 11173011), the Doctoral Program of Higher Education (20110142120037), and the CAS/SAFEA International Partnership Program for Creative Research Teams (KJCX2-YW-T23). LCH acknowledges support from the Carnegie Institution for Science, and he thanks the Chinese Academy of Sciences and the hospitality of the National Astronomical Observatories, where part of this work was done.

REFERENCES

- Abramowicz, M. A., Chen, X., Kato, S., Lasota, J.-P., & Regev, O. 1995, *ApJ*, 438, 37
- Barthel, P. D., & Arnaud, K. A. 1996, *MNRAS*, 283, L45
- Bianchi, S., Guainazzi, M., Matt, G., Fonseca Bonilla, N., & Ponti, G. 2009, *A&A*, 495, 421
- Blandford, R. D., & Begelman, M. C. 1999, *MNRAS*, 303, L1
- Blandford, R. D., & Payne, D. G. 1982, *MNRAS*, 199, 883
- Blandford, R. D., & Znajek, R. L. 1977, *MNRAS*, 179, 433
- Broderick, J. W., & Fender, R. P. 2011, *MNRAS*, 417, 184
- Buttiglione, S., Capetti, A., Celotti, A., et al. 2010, *A&A*, 509, 6
- Cao, X. 2002, *ApJ*, 613, 716
- Cao, X. 2009, *MNRAS*, 394, 207
- Cao, X. 2011, *ApJ*, 737, 94
- Corbel, S., Fender, R. P., Tzioumis, A. K., et al. 2000, *A&A*, 359, 251
- Corbel, S., Nowak, M. A., Fender, R. P., Tzioumis, A. K., & Markoff, S. 2003, *A&A*, 400, 1007
- Ding, J., Yuan, F., & Liang, E. 2010, *ApJ*, 708, 1545
- Done, C., Gierliński, M., & Kubota, A. 2007, *A&ARev.*, 15, 1
- Eracleous, M., Hwang, J. A., & Flohic, H. M. L. G. 2010, *ApJS*, 187, 135
- Falcke, H., Kording, E. G., & Markoff, S. 2004, *A&A*, 414, 895
- Fanaroff, B. L., & Riley, J. M. 1974, *MNRAS*, 167, 31P
- Fender, R. P., Corbel, S., Tzioumis, T., et al. 1999, *ApJ*, 519, L165
- Gallo, E., Fender, R. P., & Pooley, G. G. 2003, *MNRAS*, 344, 60
- Ghisellini, G., & Celotti, A. 2001, *A&A*, 379, 1
- Ghisellini, G., Padovani, P., Celotti, A., & Maraschi, L. 1993, *ApJ*, 407, 65
- Giozzi, M., Sambruna, R. M., & Eracleous, M. 2003, *ApJ*, 584, 176
- Gu, M., & Cao, X. 2009, *MNRAS*, 399, 349
- Gültekin, K., Richstone, D. O., Gebhardt, K., et al. 2009, *ApJ*, 698, 198
- Hardcastle, M. J., Evans, D. A., & Croston, J. H. 2009, *MNRAS*, 396, 1929
- Hardcastle, M. J., Harris, D. E., Worrall, D. M., & Birkinshaw, M. 2004, *ApJ*, 612, 729
- Ho, L. C. 1999, *ApJ*, 516, 672
- Ho, L. C. 2002, *ApJ*, 564, 120
- Ho, L. C. 2008, *ARA&A*, 46, 475
- Ho, L. C. 2009, *ApJ*, 699, 626
- Ho, L. C., Feigelson, E. D., Townsley, L. K., et al. 2001, *ApJ*, 549, 51
- Ho, L. C., Filippenko, A. V., & Sargent, W. L. 1995, *ApJS*, 98, 477
- Ho, L. C., Filippenko, A. V., & Sargent, W. L. 1997a, *ApJS*, 112, 315
- Ho, L. C., Filippenko, A. V., & Sargent, W. L. W. 2003, *ApJ*, 583, 159
- Ho, L. C., Filippenko, A. V., Sargent, W. L., & Peng, C. Y. 1997b, *ApJS*, 112, 391
- Ho, L. C., Greene, J. E., Filippenko, A. V., & Sargent, W. L. W. 2009, *ApJS*, 183, 1
- Ho, L. C., & Peng, C. Y. 2001, *ApJ*, 555, 650
- Ho, L. C., & Ulvestad, J. S. 2001, *ApJS*, 133, 77
- Ichimaru, S. 1977, *ApJ*, 214, 840
- Kaspi, S., Maoz, D., Netzer, H., et al. 2005, *ApJ*, 629, 61
- Kaspi, S., Smith, P. S., Netzer, H., et al. 2000, *ApJ*, 533, 631
- Kato, S., Fukue, J., & Mineshige, S. 2008, *Black-Hole Accretion Disks: Towards a New Paradigm* (Kyoto: Kyoto Univ. Press)
- Kellermann, K. I., Sramek, R. A., Schmidt, M., Green, R. F., & Shaffer, D. B. 1994, *AJ*, 108, 1163
- Laor, A., & Behar, E. 2008, *MNRAS*, 390, 847
- Li, S.-L., & Cao, X. 2012, *ApJ*, 753, 24
- Liu, H., & Wu, Q. 2013, *ApJ*, 764, 17
- Malizia, A., Landi, R., Bassani, L., et al. 2007, *ApJ*, 668, 81
- Marconi, A., & Hunt, L. K. 2003, *ApJ*, 589, L21
- McGill, K. L., Woo, J.-H., Treu, T., & Malkan, M. A. 2008, *ApJ*, 673, 703
- McLure, R. J., & Dunlop, J. S. 2004, *MNRAS*, 352, 1390
- McLure, R. J., Willott, C. J., Jarvis, M. J., et al. 2004, *MNRAS*, 351, 347
- Meier, D. L. 2001, *ApJ*, 548, L9
- Merloni, A., & Fabian, A. C. 2002, *MNRAS*, 332, 165
- Merloni, A., Heinz, S., & Di Matteo, T. 2003, *MNRAS*, 345, 1057
- Miller, J. M., Pooley, G. G., Fabian, A. C., et al. 2012, *ApJ*, 757, 11
- Nagar, N. M., Falcke, H., & Wilson, A. S. 2005, *A&A*, 435, 521
- Narayan, R., & McClintock, J. E. 2008, *New Astronomy Reviews*, 51, 733
- Narayan, R., & McClintock, J. E. 2012, *MNRAS*, 419, 69
- Narayan, R., & Yi, I. 1994, *ApJ*, 428, 13
- Narayan, R., & Yi, I. 1995, *ApJ*, 452, 710
- Nemmen, R., Storchi-Bergmann, T., Eracleous, M. 2013, *ApJ*, submitted (arXiv:1112.4640)
- Panessa, F., Bassani, L., Cappi, M., et al. 2006, *A&A*, 455, 173
- Pian, E., Romano, P., Maoz, D., et al. 2010, *MNRAS*, 401, 677
- Qiao, E., & Liu, B. F. 2013, *ApJ*, 764, 2
- Quataert, E., Di Matteo, T., Narayan, R., & Ho, L. C. 1999, *ApJ*, 525, 89
- Remillard, R. A., & McClintock, J. E. 2006, *ARA&A*, 44, 49
- Shakura, N. I., & Sunyaev, R. A. 1973, *A&A*, 24, 337
- Sikora, M., Stawarz, L., & Lasota, J.-P. 2007, *ApJ*, 658, 815
- Sobolewska, M. A., & Papadakis, I. E. 2009, *MNRAS*, 399, 1597
- Spruit, H. C. 2010, *Lecture Notes in Physics*, 794, 233
- Strateva, I. V., Brandt, W. N., Schneider, D. P., Vanden Berk, D. G., & Vignali, C. 2005, *AJ*, 130, 387
- Tchekhovskoy, A., Narayan, R., & McKinney, J. C. 2011, *MNRAS*, 418, 79
- Tremaine, S., Gebhardt, K., Bender, R., et al. 2002, *ApJ*, 574, 740
- Vestergaard, M., & Peterson, B. M. 2006, *ApJ*, 641, 689
- Wang, J.-M., Luo, B., & Ho, L. C. 2004a, *ApJ*, 615, 9
- Wang, J.-M., Watarai, K.-Y., & Mineshige, S., 2004b, *ApJ*, 607, 107
- Willott, C. J., Rawlings, S., Blundell, K. M., & Lacy, M. 1999, *MNRAS*, 309, 1017
- Wrobel, J. M., Terashima, Y., & Ho, L. C. 2008, *ApJ*, 675, 1041
- Wu, Q., & Cao, X. 2008, *ApJ*, 687, 156
- Wu, Q., Cao, X., & Wang, D. X. 2011, *ApJ*, 735, 50
- Wu, Q., & Gu, M. 2008, *ApJ*, 682, 212
- Wu, Q., Yuan, F., & Cao, X. 2007, *ApJ*, 669, 96
- Xu, C., Livio, M., & Baum, S. 1999, *AJ*, 118, 1169
- Xu, Y.-D. 2011, *ApJ*, 739, 64
- Xu, Y.-D., Cao, X., & Wu, Q. 2009, *ApJ*, 694, L107
- Younes, G., Porquet, D., Sabra, B., & Reeves, J. N. 2011, *A&A*, 530, 149
- Yu, Z., Yuan, F., & Ho, L. C. 2011, *ApJ*, 726, 87
- Yuan, F. 2007, in *The Central Engine of Active Galactic Nuclei*, ed. L. C. Ho & J.-M. Wang (San Francisco: ASP), 95
- Yuan, F., & Cui, W. 2005, *ApJ*, 629, 408

Yuan, F., Cui, W., & Narayan, R. 2005, 620, 905
Yuan, F., Quataert, E., & Narayan, R. 2003, ApJ, 598, 301
Yuan, F., Yu, Z., & Ho, L. C. 2009, ApJ, 703, 1034

Zdziarski, A. A., Skinner, G. K., Pooley, G. G., & Lubinski, P. 2011,
MNRAS, 416, 1324
Zhou, X. L., & Zhang, S. N. 2010, ApJ, 713, 11